solar

MDPI

Article

Energy Assessment as a Decision-Making Framework for the Selection and Sizing of Solar Technologies by Energy Vector in Buildings: A Case Study of a University Residence Hall

Hilja Ndapewa Kaapanda [1], José Pedro Monteagudo Yanes [1], Julio Rafael Gómez Sarduy [1], Mariano Garduño-Aparicio [2], Yoisdel Castillo Alvarez [3,*], Reinier Jiménez Borges [4], Suresh Thenozhi [2,*], Luis Angel Iturralde Carrera [2] and Juvenal Rodríguez-Reséndiz [2]

[1] Center for Energy and Environmental Studies (CEEMA), Faculty of Engineering, "Carlos Rafael Rodríguez" University of Cienfuegos, Cienfuegos 59430, Cuba; hilja.ta@gmail.com (H.N.K.); jgomez@ucf.edu.cu (J.R.G.S.)
[2] Facultad de Ingeniería, Universidad Autónoma de Querétaro, Santiago de Querétaro 76010, Mexico; liturralde28@alumnos.uaq.mx (L.A.I.C.); juvenal@uaq.edu.mx (J.R.-R.)
[3] Department of Mechanical Engineering, Universidad Tecnológica del Perú, Lima 15046, Peru
[4] Department of Mechanical Engineering, Faculty of Engineering, Universidad de Cienfuegos "Carlos Rafael Rodríguez", Cienfuegos 59430, Cuba; rjimenezborges@gmail.com
* Correspondence: c19773@utp.edu.pe (Y.C.A.); suresh@uaq.mx (S.T.)

Abstract

The sizing of rooftop solar energy systems is commonly based on the most visible load or on generic end-use allocations, leading to an inadequate distribution of the limited rooftop area between heat and electricity. This study formalizes the energy audit within a three-level deterministic framework that selects and sizes solar technologies by energy vector: demand is first decomposed by vector; the technology for the thermal vector is then selected through a levelized cost of heat selection ratio ψ, while the photovoltaic system of the electrical vector is sized for self-consumption; and the rooftop area is finally allocated among vectors according to marginal value per unit area. In a 75-bed university residence in Cienfuegos, Cuba, air conditioning is the dominant energy end-use in terms of installed power (accounting for 77% of the connected load), whereas the thermal vector dominates annual energy consumption (domestic hot water: 127,440 versus 76,818 kWh/year for electricity; thermal-to-electric ratio 1.66). Solar thermal technology has been selected for the thermal vector (0.018 versus 0.088 USD/kWh$_{th}$; $\psi = 0.21$, a robust value according to the sensitivity analysis), and the marginal value (≈111 versus ≈32 USD/(m^2·year)) allocates 104 m^2 to solar thermal collectors and 134 m^2 to photovoltaic energy, thereby reversing the original design that prioritized photovoltaic energy. The resulting portfolio achieves an annual solar fraction close to 100% in both vectors on an energy balance basis, avoids 86.5 t of operational CO_2 emissions per year, and combines a simple payback of 1.1 years (solar thermal) with a net present value of 55,327 USD and an internal rate of return of 28% (photovoltaics). The sizing decision is shown to be robust to the choice of statistical design criterion (median, mean, P90, maximum), and none of the three framework decisions is reversed under ±30% parameter variations. By replacing the subjective weightings of multi-criteria methods with observable economic criteria, the framework provides a replicable and auditable design protocol.

Keywords: energy audit; energy vector; solar technology selection; levelized cost of heat; marginal value allocation; solar thermal; photovoltaics; techno-economic assessment; energy performance indicators; buildings

Check for updates

Academic Editors: Andreu Moià-Pol and Iván Alonso de Miguel

Received: 21 June 2026
Revised: 7 July 2026
Accepted: 22 July 2026
Published: 24 July 2026

1. Introduction

The building sector is one of the world's largest consumers of energy and sources of carbon emissions: according to the latest Global Status Report for Buildings and Construction, buildings accounted for approximately 32% of global energy demand and nearly 34% of energy-related CO_2 emissions in 2023 [1]. In this context, the integration of distributed renewable generation into buildings has emerged as one of the most direct pathways to decarbonize the built environment while simultaneously reducing pressure on fragile or carbon-intensive electrical grids [2,3]. A distinctive feature of building energy demand is that it is not a homogeneous quantity, but rather is distributed across at least two physically distinct energy vectors: electricity—lighting, appliances, pumping, and increasingly air conditioning—and low-temperature heat, dominated by domestic hot water (DHW). Solar energy can supply both vectors at the point of use through photovoltaic (PV) modules for the electrical vector and solar thermal collectors for the thermal vector, making it a particularly suitable resource in regions combining high solar irradiation with constrained electrical systems [4]. This combination is characteristic of small island states and isolated territories, whose dependence on imported fuels, limited generation capacity, and weak grids have been extensively documented [5–7]; it is not claimed to be universal across developing countries—large economies such as India or Brazil possess extensive interconnected systems—so the operational context targeted by this work is specifically that of island and weak-grid settings.

The literature has extensively documented the application of solar technologies in buildings. In the electrical vector, beyond conventional rooftop PV systems, studies have examined building-integrated photovoltaics (BIPVs) in façades and photovoltaic systems combined with green roofs [8,9], as well as design and sizing tools for distributed photovoltaic generation [10]. Within university and residential settings—the context of interest in the present work—several case studies have evaluated the photovoltaic potential of campus buildings and student residences under different climatic and economic conditions [11–14]. In the thermal vector, solar water heaters for domestic hot water (DHW) have demonstrated significant reductions in energy consumption and emissions in buildings [15,16], while solar-assisted heat pump systems have gained prominence as an alternative for low-temperature heat supply [17–19]. Complementarily, hybrid photovoltaic–thermal (PVT) technologies and solar systems coupled with heat pumps enable the simultaneous supply of electrical and thermal vectors, including in residential buildings [20–24].

To orient these decisions, research has frequently relied on multi-criteria decision-making (MCDM) methods such as AHP and TOPSIS. However, their application has predominantly focused on a different problem: the selection of sites for large-scale solar plants, weighing climatic, technical, geographic, and economic criteria [25–28]. When the MCDM approach has been brought to the building scale, it has typically addressed product selection—for example, choosing the best photovoltaic module on the market for a specific client [29]—or the holistic assessment of solar potential on urban surfaces [30], rather than the selection among solar technologies serving different demand vectors. Decision frameworks for building energy and photovoltaics also exist, but they are largely monovectorial: they optimize the orientation and number of PV panels to maximize self-consumption relative to electrical demand [31], or support energy planning at the urban scale [3], without addressing the allocation between technologies across vectors.

Furthermore, energy auditing—formalized in energy management systems such as the ISO 50001 standard [32]—is the established instrument for characterizing consumption, setting the energy baseline, and identifying improvement measures [33,34]; however, its output is rarely translated into a structured and reproducible decision rule on which solar technology to install, for which vector, and in what proportion.

In the thermal vector, in particular, the competition between solar thermal systems and PV coupled with heat pumps has been analyzed in detail from a techno-economic and performance perspective [35,36], but these comparisons are conducted as standalone studies rather than as an integrated step within a building-scale decision-making procedure. The closest work to the present study is that of Bosu et al. [16], who carried out an energy audit of a university residential building and evaluated the integration of PV and solar water heating from techno-economic and environmental perspectives, reporting savings for both technologies. However, that study remains an evaluation: it sizes and assesses both technologies in parallel and quantifies their energy, economic, and environmental performance, but it does not transform this assessment into a decision mechanism. There is no explicit rule that uses the outputs of the audit to select between technologies within the same vector—for example, solar thermal versus PV-plus-heat-pump for domestic hot water (DHW)—nor to allocate a constrained resource such as roof area or capital between the electrical and thermal vectors. More broadly, no existing framework treats the energy audit as a multilevel decision engine that, starting from data already produced by a standard audit, selects and sizes a portfolio of solar technologies organized by energy vector.

This study addresses that gap. It proposes a decision framework in which the energy audit operates at three levels: (i) characterization and decomposition of demand by energy vector; (ii) selection of the most suitable solar technology within each vector—including intravector competition between thermal alternatives—through an explicit levelized cost criterion weighted by the building's operational context; and (iii) arbitration among competing technologies under roof area or capital constraints, based on marginal value. The contribution is therefore threefold: (i) the energy audit is formalized as a decision engine rather than a purely diagnostic instrument; (ii) intravector selection is governed by an explicit and reproducible levelized cost ratio instead of subjective expert weights; and (iii) intervector allocation of the scarce roof area is resolved by marginal value per unit surface, so that every design decision is traceable to audit variables. None of these tools is new in isolation—energy auditing, levelized costing, PV sizing, and marginal analysis are all established instruments; the methodological novelty lies in their chaining into a single deterministic, auditable decision protocol organized by energy vector, a combination absent from the literature reviewed above.

The framework is demonstrated on the postgraduate residence of the University of Cienfuegos (Cuba), a building whose simultaneous electricity and DHW demand, together with an operational context characterized by resource constraints and dependence on imported fuels, makes it a suitable case for vector-based decision-making. Cuba is also a particularly relevant setting: with approximately 95% of its electricity generated from fossil fuels and a target of 24% renewable energy by 2030, the country is undergoing an energy transition in which solar utilization in buildings plays a strategic role [37–42]. It is emphasized that the study is presented as a single-case demonstration of the framework, not as a typological validation: the contribution is methodological—the formalization of the transition from diagnosis to decision—and the case serves to illustrate its operation and plausibility rather than to establish statistical generalization.

Accordingly, the general objective of this work is to formulate and demonstrate an energy-audit-based decision framework for the selection and sizing of solar technologies by energy vector in buildings.

The remainder of this paper is organized as follows. Section 2, Materials and Methods, describes the case study building and its audit data, and formalizes the three-level decision framework: decomposition of demand by energy vector, intravector technology selection through the levelized cost of heat, and intervector allocation of the constrained roof area by marginal value. Section 3, Results, applies the framework to the postgraduate residence, reporting the energy audit, the technology selection for each vector, the allocation of the roof surface, the techno-economic, environmental, and energy performance indicators of the resulting portfolio, and the sensitivity analysis. Section 4, Discussion, interprets the findings, positions the framework with respect to the literature on solar technology assessment and selection in buildings, and delimits its scope and limitations. Finally, Section 5, Conclusions, summarizes the main findings, the methodological contribution, and future research directions.

2. Materials and Methods

2.1. Case Study and Diagnostic Data

The framework is demonstrated on the postgraduate residence of the University of Cienfuegos (Cuba; latitude $\Phi = 22.0°$ N), a four-story building constructed in concrete and masonry with 27 rooms, 19 bathrooms, and a lodging capacity of 75 people. The facility also operates as a dining installation and, during vacation periods, as a higher education guest residence. The selection of this case is justified by the fact that the building exhibits simultaneously non-negligible electrical and domestic hot water (DHW) thermal demands, a necessary condition for a non-trivial vector-based decision problem.

The diagnostic data were obtained through load inventory, utility meter readings, and normative estimates of DHW consumption, and are summarized in Table 1. It should be noted that two inconsistencies present in the primary source are explicitly addressed in the analysis: (i) the electrical consumption estimated from the load inventory/software (≈4516 kWh/month) differs from the maximum meter reading (8224 kWh/month, May); therefore, the maximum measured value is adopted as the design demand, while the range is reported; and (ii) the annual thermal demand is of the same order of magnitude as the annual electrical demand, which assigns the thermal vector a first-order, rather than marginal, relevance.

Table 1. Energy audit data of the building (postgraduate residence, University of Cienfuegos).

Variable	Value	Observation
Connected electrical load	114.93–116.03 kW	inventory/software
Monthly electricity consumption (meter reading)	4015–8224 kWh/month	min. Nov./max. May
Design electrical demand, $E_{el,d}$	8224 kWh/month (≈274 kWh/day)	peak envelope
Air conditioning share	≈77 % of load	electrical vector
DHW demand, V_{ACS}	8700 L/day	6000 (residential) + 2700 (kitchen)
Usage/inlet temperature, T_{set}/T_{in}	60/25 °C	$\Delta T = 35$ °C
Thermal demand, E_{th}	≈354 kWh_{th}/day	Equation (1)
Peak sun hours, HSP	5 h/day	10:30–15:30
Global irradiation, H	5.64–5.81 kWh/m^2/day	≈1500–1700 kWh/m^2/year
Average ambient temperature	27–28.5 °C	tropical climate
Usable roof area, A_{roof}	236.99 m^2 (main) + auxiliary roofs	gross 279.31 m^2 minus 1-m maintenance corridor; tilt $\beta = 22°$, azimuth 0°; auxiliary: two adjacent buildings, same orientation

Regarding data vintage, the meter readings correspond to September 2016–May 2017, the most recent complete series available for the building; they predate the post-2019 supply disruptions of the Cuban electrical system and therefore represent an unconstrained-demand operating regime, which is the appropriate reference for capacity sizing. The framework requires one representative year of normal operation rather than real-time data, and the influence of the proportionally estimated summer quarter on the decision variables is quantified in the sensitivity analysis (Section 3.5).

2.2. General Structure of the Decision Framework

The proposed framework reinterprets the energy audit as a decision engine operating at three sequential levels. Level 1 characterizes and decomposes demand by energy vector and quantifies solar resource availability and physical constraints. Level 2 selects, within each vector, the most suitable solar technology using a context-adjusted levelized cost criterion, explicitly resolving intravector competition in the thermal vector (solar thermal versus photovoltaic coupled with heat pumps). Level 3 arbitrates between the selected technologies when roof area or capital is insufficient to fully satisfy the target demand, allocating the scarce resource based on marginal value. The output is a vector-based solar portfolio (technology, proportion, and sizing by energy vector) that is fully traceable to diagnostic variables. Figure 1 summarizes this decision flow.

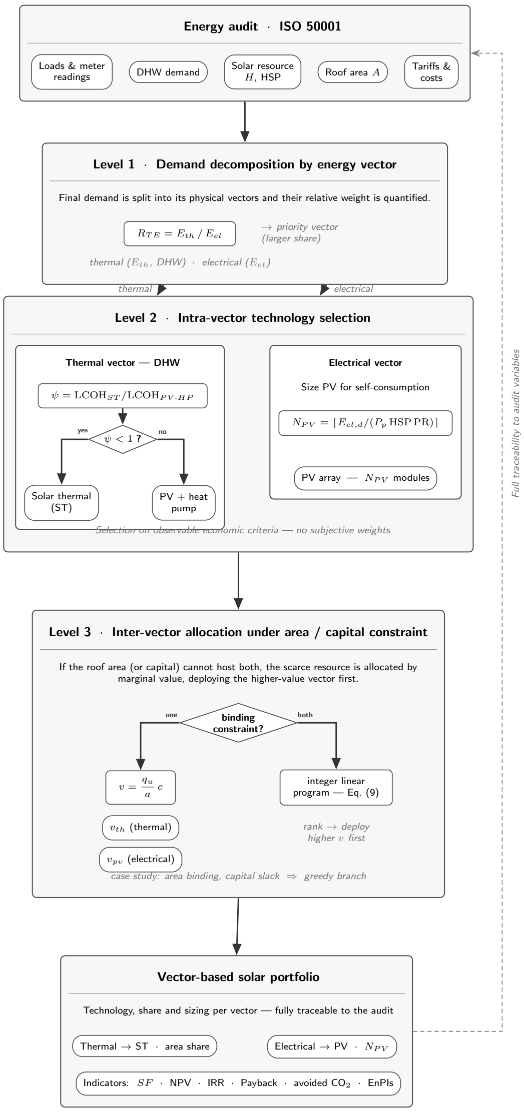

Figure 1. Three-level decision framework based on the energy audit. Starting from ISO 50001 audit data, Level 1 decomposes demand by energy vector and computes the thermal-to-electrical ratio R_{TE};

Level 2 selects the technology within each vector using the levelized cost of heat and the coefficient ψ (and sizes the PV system for the electrical vector); and Level 3 allocates the scarce resource (area or capital) based on marginal value v. The output is a vector-based solar portfolio, fully traceable to the audit and evaluated through solar fraction, NPV, IRR, payback period, avoided CO_2 emissions, and energy performance indicators.

2.3. Level 1: Characterization and Decomposition of Demand by Vector

The demand is divided into two vectors: the electrical vector, E_{el} (kWh/year), obtained from the load inventory and utility meter readings, and the domestic hot water

(DHW) thermal vector, E_{th} ($\mathrm{kWh_{th}/year}$), determined from the required water volume as Equation (1):

$$E_{th} = \frac{\rho\, c_p\, V_{ACS}\, (T_{set} - T_{in})}{\eta_{dist}}, \tag{1}$$

where $\rho = 1000\ \mathrm{kg/m^3}$ is the water density, $c_p = 4.18\ \mathrm{kJ/(kg\,^\circ C)}$ its specific heat capacity, V_{ACS} is the daily water demand, T_{set} and T_{in} are the set-point and inlet temperatures, and η_{dist} is the distribution/storage efficiency.

The primary structural indicator is the thermal-to-electrical ratio Equation (2):

$$R_{TE} = \frac{E_{th}}{E_{el}}, \tag{2}$$

which quantifies the relative weight of both vectors and guides priority allocation.

Additionally, the solar resource is characterized through global irradiation H and peak sun hours (HSP), the usable roof area A_{roof} (including orientation, tilt, and shading conditions), and the techno-economic and operational context (electricity tariff, displaced fuel cost, import dependency, and operation and maintenance capacity). These constitute the input variables for Levels 2 and 3 of the decision framework.

2.4. Level 2: Intravector Technology Selection Procedure

2.4.1. Thermal Vector: Levelized Cost of Heat Criterion

For the thermal vector, solar thermal (ST) collectors compete with photovoltaic systems coupled to heat pumps (PV-HPs), both of which are capable of meeting the domestic hot water (DHW) demand. The comparison is performed using the levelized cost of heat (LCOH), defined for a given technology j as Equation (3):

$$\mathrm{LCOH}_j = \frac{\mathrm{CRF}(i,n)\, C_{\mathrm{inv},j} + C_{\mathrm{O\&M},j}}{Q_{u,j}}, \qquad \mathrm{CRF}(i,n) = \frac{i\,(1+i)^n}{(1+i)^n - 1}, \tag{3}$$

where $C_{\mathrm{inv},j}$ is the investment cost, $C_{\mathrm{O\&M},j}$ is the annual operation and maintenance cost, $Q_{u,j}$ is the annual useful heat delivered, CRF is the capital recovery factor, i is the discount rate, and n is the lifetime horizon.

For the PV-HP system, the electricity required to supply the covered heat demand Q_{cov} is obtained from the seasonal coefficient of performance $\mathrm{COP_{est}}$ Equation (4):

$$E_{el,\mathrm{HP}} = \frac{Q_{\mathrm{cov}}}{\mathrm{COP_{est}}}, \tag{4}$$

so that its investment cost includes both the photovoltaic array sized to supply $E_{el,\mathrm{HP}}$ and the heat pump unit.

Instead of a discretionary adjustment factor, monetizable contextual constraints are directly incorporated into the cost terms of Equation (3): the investment cost is adjusted to account for import surcharges of equipment not manufactured locally, and O&M and unavailability costs reflect local tariffs and service reliability at the site. The primary decision is therefore purely economic and reproducible: the selection ratio is defined as Equation (5):

$$\psi = \frac{\mathrm{LCOH_{ST}}}{\mathrm{LCOH_{PV\text{-}HP}}}, \qquad \text{select} \begin{cases} \mathrm{ST} & \text{if } \psi < 1, \\ \text{PV-HP} & \text{if } \psi \geq 1. \end{cases} \tag{5}$$

2.4.2. Robustness Layer (Non-Monetizable Attributes)

For strategic attributes that cannot be directly translated into cost (import dependency, local maintainability, and technological maturity in the given context), a transparent and reproducible robustness index is constructed Equation (6):

$$R_b = \sum_k w_k\, s_k, \qquad \sum_k w_k = 1, \quad s_k \in [0,1], \tag{6}$$

where s_k is the normalized score of attribute k and w_k its weight. This index does not replace Equation (5); it is only used as a tie-breaker when levelized costs are statistically indistinguishable ($|\,\psi - 1\,|$ below a predefined threshold) and is, in all cases, subjected to sensitivity analysis to verify decision stability. This separation between the economic criterion (hard and reproducible) and the strategic adjustment (explicit and bounded) avoids the bias of an ad hoc multiplier.

2.4.3. Electrical Vector

For the electrical vector, a photovoltaic (PV) system is adopted, sized to maximize self-consumption under area and capital constraints. The number of modules is determined from the design daily demand $E_{el,d}$, the module peak power P_p, peak sun hours (HSP), and the system performance ratio (PR) [43–46], Equation (7):

$$N_{PV} = \left\lceil \frac{E_{el,d}}{P_p\,\mathrm{HSP\,PR}} \right\rceil, \tag{7}$$

bounded above by the maximum number of modules that can be accommodated within the available area [46–49] (Equation (11)). Equation (7) evaluated at the design (peak envelope) demand defines the upper sizing bound; the deployed number of modules is the minimum of this value and the area bound of Equation (11), and its robustness to the statistical criterion used for $E_{el,d}$ (median, mean, P90, maximum).

2.5. Level 3: Intervector Allocation Under Constraints

When roof area or capital is insufficient to fully size both technologies to their target demand, the scarce resource is allocated based on marginal value, i.e., the avoided cost per unit of consumed resource, Equation (8). For the thermal and electrical vectors, respectively:

$$v_{th} = \frac{q_u}{a_{\mathrm{ST}}}\, c_{th}, \qquad v_{pv} = \frac{e_{pv}}{a_{\mathrm{PV}}}\, c_{el}, \tag{8}$$

where q_u and e_{pv} are the annual useful heat and electricity per unit (collector or module), a_{ST} and a_{PV} are their respective area footprints, and c_{th} and c_{el} are the unit costs of the displaced thermal and electrical energy.

The rule assigns the resource preferentially to the technology with the highest marginal value until either area or capital is exhausted. In the general case where both constraints are active, the problem is formulated as a linear allocation that maximizes total avoided cost (or, alternatively, avoided emissions) subject to area and capital constraints; see Equation (9):

$$\max_{x_{\mathrm{ST}},\, x_{\mathrm{PV}}} \sum_j v_j\, x_j \quad \text{s.t.} \quad \sum_j a_j\, x_j \le A_{roof}, \ \sum_j c_{\mathrm{inv},j}\, x_j \le C_{\max}, \ \ x_j \in \mathbb{Z}^+, \tag{9}$$

whose solution coincides with the greedy allocation based on marginal value when only one constraint is active.

2.6. Sizing of the Solar Field and Performance Indicators

The number of solar collectors is obtained from the required DHW volume and the unit production of a collector $q_{V,\text{col}}$; see Equation (10):

$$N_{\text{ST}} = \left\lceil \frac{V_{ACS}}{q_{V,\text{col}}} \right\rceil, \tag{10}$$

while the maximum number of units (modules or collectors) that can be installed on the roof is determined geometrically from the usable area and the unit footprint a, accounting for row spacing $d = L \sin\beta \cdot k$ (with k the spacing factor) to avoid inter-row shading; see Equation (11):

$$N_{\max} = \left\lfloor \frac{A_{roof}}{a} \right\rfloor. \tag{11}$$

Performance is evaluated through the solar fraction of each vector, $SF = Q_{\text{solar}}/E_{\text{demand}}$, as well as energy performance indicators (specific consumption before and after the intervention). Economic evaluation uses the net present value (NPV), Equation (12), internal rate of return (IRR), and payback period (PBP):

$$\text{NPV} = -C_{\text{inv}} + \sum_{t=1}^{n} \frac{CF_t}{(1+i)^t}, \qquad \text{IRR}: \ \text{NPV}(i^*) = 0, \tag{12}$$

where CF_t is the cash flow in year t (energy savings minus O&M costs). Finally, environmental performance is quantified through avoided CO_2 emissions; see Equation (13):

$$\Delta\text{CO}_2 = E_{\text{saved}} \cdot FE, \tag{13}$$

where E_{saved} is the displaced energy (electric or thermal) and FE is the emission factor of the substituted source (electric grid or fuel). In this study, $FE = 0.608$ kg CO_2/kWh is adopted for the oil-dominated Cuban grid, consistent with the country-level emission factors reported by the International Energy Agency [50], and $FE = 2.68$ kg CO_2/L for diesel combustion, consistent with IPCC default factors for stationary combustion [51]. Avoided emissions therefore quantify operational emissions only; embodied (life-cycle) emissions from equipment manufacturing and replacement are outside the system boundary [52]. All indicators are reported by vector and for the resulting portfolio, ensuring full traceability of decisions back to the diagnostic stage.

3. Results

The framework is applied to the postgraduate residence of the University of Cienfuegos, whose input data are summarized in Table 1 of Section 2. Monetary values are expressed in United States dollars (USD), with the parity 1 Cuban convertible peso = 1 USD adopted from the primary source. Results are organized according to the three levels of the framework—diagnosis, selection, and allocation—and conclude with performance indicators and a sensitivity analysis.

3.1. Energy Audit of the Building

The energy audit constitutes the first level of the framework and the foundation for all subsequent decisions. Its purpose is to establish how much energy the building consumes, in which vector, where the load is concentrated, and against which reference the intervention will be evaluated.

3.1.1. Electrical Consumption Profile

The starting point is the quantification of the magnitude and seasonality of electrical demand, which simultaneously determines the sizing baseline and the operational usage pattern of the facility. Figure 2 presents the monthly electrical consumption recorded by the building's utility meter.

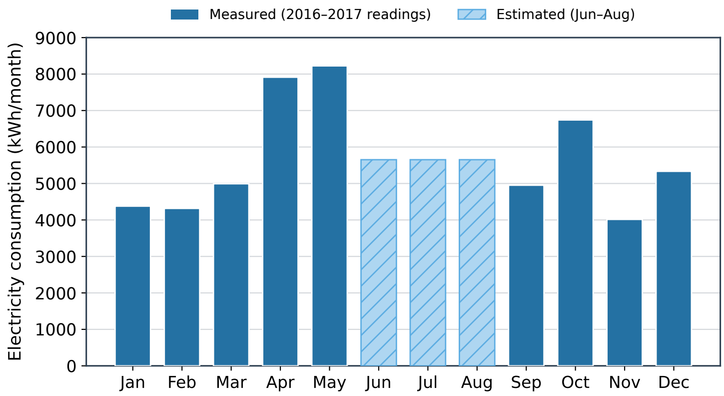

Figure 2. Monthly electrical consumption profile of the residence. Meter readings (2016–2017) are complemented with a proportional estimate for the missing summer quarter (striped bars); the maximum value in May (8224 kWh) is used as the system sizing baseline.

Consumption ranges from 4015 kWh in November to 8224 kWh in May; the maximum occurs at the beginning of the warm season, linking peak demand to air-conditioning use. The nine available readings (September 2016–May 2017) are 4952, 6741, 4015, 5333, 4378, 4316, 4992, 7913, and 8224 kWh/month, with a median of 4992 kWh/month, a mean of 5652 kWh/month, and an empirical P90 of 7975–8224 kWh/month depending on the interpolation method—statistically indistinguishable from the observed maximum, as expected for a sample of $n = 9$. Based on nine available readings and a proportional estimate of the missing summer quarter, the annual electrical demand amounts to E_{el} = 76,818 kWh/year, equivalent to a specific consumption of approximately 1024 kWh per bed per year. The May peak value is adopted as the design basis for the photovoltaic system. This value defines the design envelope only; the consequences of alternative statistical sizing criteria, and the reason why the envelope does not translate into oversizing, are quantified in Section 3.2.

3.1.2. Electrical Load Characterization

Once the consumption magnitude is established, the audit identifies its composition: where the load is concentrated and which end-uses dominate, information that defines the significant energy use to be targeted. Figure 3 decomposes the connected electrical load by floor (a) and by equipment type through a Pareto diagram (b).

The total connected load is 114.93 kW, a value consistent with the 116.03 kW obtained independently using the Audipre software version 2.1 [53]. The Pareto diagram shows that air conditioning alone accounts for approximately 77% of the load (≈88.5 kW): it constitutes the significant energy use of the electrical vector, while the first six equipment categories account for approximately 96%. By floor, the third (≈36 kW) and fourth (≈35 kW) floors concentrate approximately 61% of the load, associated with triple rooms and suites. The average building demand (≈8.8 kW) represents only 7.6% of the connected load—equivalent to 668 full-load hours per year—highlighting the low simultaneity typical of hotel-type occupancy. The installation operates at low voltage, 110 V single-phase.

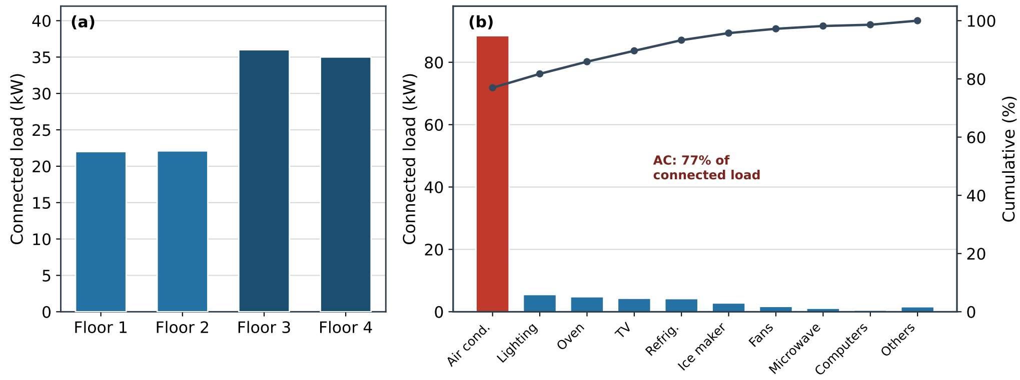

Figure 3. Characterization of the connected electrical load. (**a**) Distribution by floor: the third and fourth floors account for approximately 61% of the load. (**b**) Pareto chart by equipment type: air conditioning accounts for approximately 77% of the connected load (the line indicates cumulative percentage).

3.1.3. Demand by Vector

The audit is completed by contrasting the two energy vectors of the building, since their relative weight determines the most appropriate direction for solar deployment. In addition to electrical demand, the thermal demand for domestic hot water (DHW) is considered. With 8700 L/day at 60 °C ($\Delta T = 35$ °C), and according to Equation (1) (with $\eta_{dist} = 1$, since distribution and storage losses were not metered separately in the primary source; the effect of $\eta_{dist} < 1$ on the decision variables is quantified in Section 3.5), the thermal demand is as follows:

$$E_{th} = \rho\, c_p\, V_{ACS}\, \Delta T = \frac{1000 \times 4.18 \times 8.7 \times 35}{3600} \approx 354\ \mathrm{kWh_{th}/day} \approx 127{,}440\ \mathrm{kWh_{th}/year}.$$

Figure 4 and Table 2 present the decomposition of final energy demand by vector.

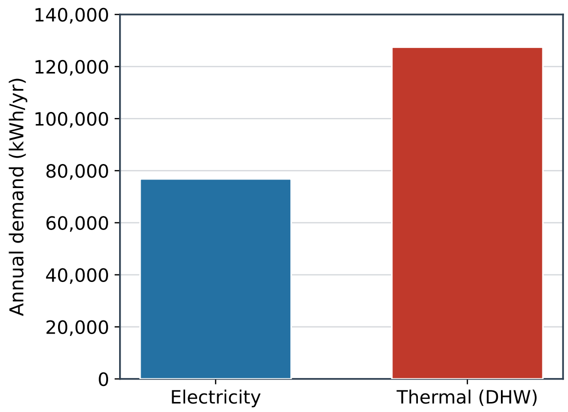

Figure 4. Decomposition of annual energy demand by vector. The thermal vector (DHW) represents 62.4% and the electrical vector 37.6%, with a thermal-to-electrical ratio $R_{TE} = 1.66$.

Table 2. Level 1. Decomposition of energy demand by energy vector.

Vector	Annual Demand	Share
Electrical, E_{el}	76,818 kWh/year	37.6%
Thermal (DHW), E_{th}	127,440 $\mathrm{kWh_{th}}$/year	62.4%
Thermal-to-electrical ratio, R_{TE}	1.66	

The thermal-to-electrical ratio (Equation (2)) is $R_{TE} = 1.66$: the thermal vector accounts for 62.4% of final demand, compared to 37.6% for the electrical vector. The thermal vector is therefore dominant, and solar deployment priority is oriented toward domestic hot water.

3.1.4. Energy Baseline

The final element of the audit is the baseline: the reference supply condition against which the solar portfolio will be evaluated. The current supply is entirely fossil-based—grid electricity for the electrical vector and diesel combustion for DHW production. Figure 5 breaks down its cost and emissions by vector, while Tables 3 and 4 summarize its parameters and performance indicators.

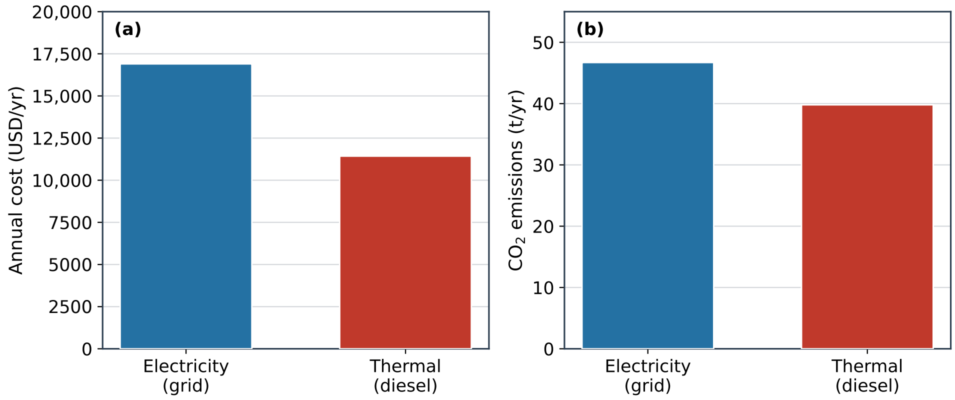

Figure 5. Energy baseline of the building. (**a**) Annual energy cost by vector, total approximately 28,329 USD/year; (**b**) annual CO_2 emissions by vector, total approximately 86.5 t/year.

Table 3. Energy baseline of the building derived from the load inventory (Figure 3).

Parameter	Electrical Vector	Thermal Vector (DHW)
Installed connected load	114.93 kW	—
Significant energy use	Air conditioning (77%)	—
Annual demand	76,818 kWh	127,440 kWh_{th}
Load factor	7.6% (668 h/year)	—
Supply source	National grid electricity	Diesel boiler (14,843 L/year)
Annual cost (USD)	16,900	11,429
Annual emissions (t CO_2)	46.7	39.8
Totals	28,329 USD/year | 86.5 t CO_2/year	

Table 4. Baseline energy performance indicators (referenced to 75 beds).

Baseline Indicator	Value
Specific electrical consumption	1024 kWh/bed·year
Specific thermal consumption (DHW)	1699 kWh_{th}/bed·year
Total energy intensity	2723 kWh/bed·year
Specific energy cost	378 USD/bed·year
Specific emissions	1153 kg CO_2/bed·year
25-year cumulative cost	708,225 USD
25-year cumulative emissions	2162 t CO_2

Grid electricity costs 16,900 USD/year and emits 46.7 t CO_2/year; the diesel boiler, consuming 14,843 L/year, costs 11,429 USD/year and emits 39.8 t CO_2/year, applying the emission factors defined in Section 2.6 (0.608 kg CO_2/kWh for the grid and 2.68 kg CO_2/L for diesel). The baseline totals 28,329 USD/year and 86.5 t CO_2/year. Referring to the 75-bed capacity, this corresponds to a specific cost of 378 USD and approximately 1153 kg CO_2 per bed per year, with a cumulative cost of approximately 708,000 USD over 25 years (Table 4). This serves as the reference against which savings and avoided emissions are quantified.

3.2. Level 2: Intravector Technology Selection

Once the thermal vector has been identified as the priority, the second level of the framework selects the technology that will supply it at the lowest cost. Using the levelized cost of heat (Equation (3)), solar thermal (ST) collectors and photovoltaic systems coupled to heat pumps (PV-HPs) are compared under a discount rate $i = 16.35\%$, a lifetime $n = 25$ years (CRF $= 0.167$), O&M costs equal to 2% of the investment, and a common useful heat output Q_u = 127,440 kWh$_{\text{th}}$/year.

The ST option uses 23 evacuated tube collectors (investment: 12,328 USD), while the PV-HP configuration, sized with $\text{COP}_{\text{est}} = 3.0$, requires a PV field of approximately 117 modules plus a 30 kW heat pump unit, totaling approximately 60,000 USD. Figure 6 and Table 5 present the resulting levelized costs:

$$\text{LCOH}_{\text{ST}} = \frac{0.167 \times 12328 + 0.02 \times 12328}{127440} \approx 0.018\ \text{USD/kWh}_{\text{th}},$$
$$\text{LCOH}_{\text{PV-HP}} = \frac{0.167 \times 60000 + 0.02 \times 60000}{127440} \approx 0.088\ \text{USD/kWh}_{\text{th}}.$$

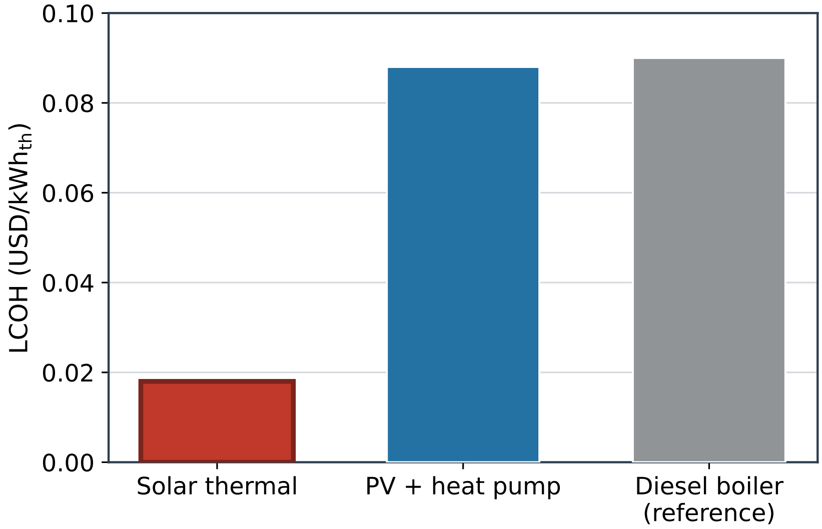

Figure 6. Levelized cost of heat (LCOH) of competing technologies for the thermal vector. Solar thermal (highlighted bar) is selected, with 0.018 USD/kWh$_{\text{th}}$ versus 0.088 for PV-HP ($\psi \approx 0.21$); the diesel boiler is included as a reference baseline.

Table 5. Level 2. Technology selection in the thermal vector.

Option	Investment (USD)	LCOH (USD/kWh$_{\text{th}}$)	Decision
Solar thermal (ST)	12,328	0.018	selected ($\psi < 1$)
PV + heat pump	≈60,000	0.088	rejected
Diesel boiler (baseline)	—	0.090	reference

The levelized cost of heat for the solar thermal option is 0.018 USD/kWh$_{\text{th}}$, compared to 0.088 USD/kWh$_{\text{th}}$ for the PV-HP system; the ratio $\psi = \text{LCOH}_{\text{ST}}/\text{LCOH}_{\text{PV-HP}} \approx 0.21 < 1$ determines the selection of solar thermal. In both technologies, the capital cost term accounts for approximately 89% of the levelized cost, while the diesel boiler reference stands at 0.090 USD/kWh$_{\text{th}}$.

For the electrical vector, Equation (7) applied to the peak envelope demand ($E_{el,d} = 274$ kWh/day, $P_p = 250$ Wp, HSP $= 5$ h/day, PR $= 0.8$) yields an upper sizing bound of $N_{PV} = 274$ modules. The deployed fleet, bounded by the area available on the main and auxiliary roofs (Equation (11)), comprises 220 modules of 250 Wp generating approximately 80,300 kWh/year, i.e., 104.5% of the annual electrical demand on an energy balance basis. Table 6 compares alternative statistical sizing criteria for the design demand: the deployed fleet lies between the annual mean sizing (211 modules) and the peak envelope (274 modules), only 4.3% above the former, so the adoption of the maximum as a design basis does not translate into oversizing—the physical area constraint truncates the peak envelope before it produces overcapacity. Moreover, with only nine monthly readings, the empirical P90 coincides in practice with the maximum, so a probability-based sizing criterion converges to the same design value, whereas a parametric P90 would lack sample support at $n = 9$.

Table 6. Comparison of statistical sizing criteria for the photovoltaic fleet (Equation (7); 250-Wp modules, HSP = 5 h/day, PR = 0.8; annual demand E_{el} = 76,818 kWh/year).

Sizing Criterion	$E_{el,d}$ (kWh/day)	N_{PV}	Generation (kWh/year)	Annual Coverage
Median of readings (P50)	166.4	167	60,955	79.3%
Mean of readings	188.4	189	68,985	89.8%
Annual mean ($E_{el}/365$)	210.5	211	77,015	100.3%
Empirical P90 ($n = 9$)	265.8–274.1	266–274	97,090–100,010	126–130%
Maximum (May; design envelope)	274.1	274	100,010	130.2%
Deployed fleet (area-bounded)	—	220	80,300	104.5%

3.3. Level 3: Intervector Allocation Under Roof Area Constraints

The third level resolves the competition for roof space. Since the available surface ($A_{roof} \approx 237$ m^2) does not simultaneously accommodate the full photovoltaic field and the solar thermal collectors, the area becomes an active constraint and is allocated according to the marginal value of each technology per unit of surface (Equation (8)).

With q_u = 5541 kWh$_{\mathrm{th}}$/year and a footprint $a_{\mathrm{ST}} \approx 4.5$ m^2 per collector, and $e_{pv} = 365$ kWh/year with $a_{\mathrm{PV}} = 2.52$ m^2 per module, Figure 7 and Table 7 report the resulting marginal values:

$$v_{th} = \frac{5541}{4.5} \times 0.090 \approx 111\ \mathrm{USD/m^2/year}, \qquad v_{pv} = \frac{365}{2.52} \times 0.22 \approx 32\ \mathrm{USD/m^2/year}.$$

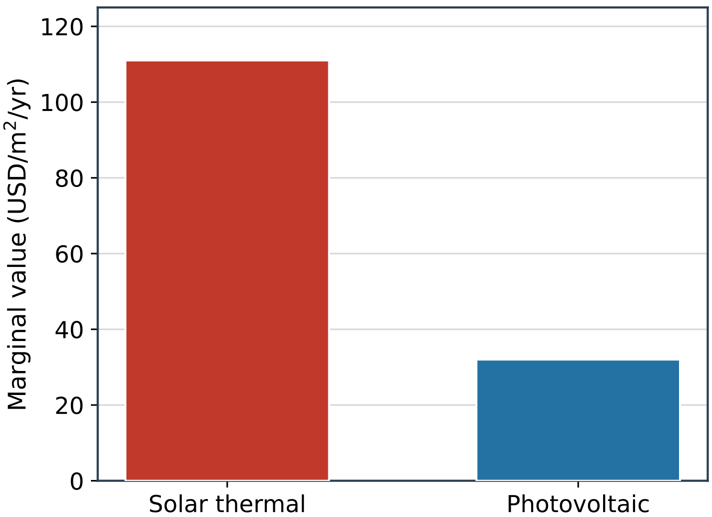

Figure 7. Marginal value per unit of roof area for each technology. Solar thermal (≈111 USD/m^2/year) exceeds photovoltaic (≈32) by a factor of approximately 3.5, determining priority allocation of the constrained roof area.

Table 7. Level 3. Marginal value per area and allocation of the main roof surface.

Technology	Marginal Value (USD/m^2/year)	Roof Priority
Solar thermal	≈111	1st (priority)
Photovoltaic	≈32	2nd (residual + auxiliary areas)

The solar thermal system yields approximately 111 USD/m^2/year compared to 32 USD/m^2/year for photovoltaics, a factor of approximately 3.5. Therefore, the main roof surface is primarily allocated to the 23 solar thermal collectors (approximately 104 m^2); the remaining area (approximately 134 m^2) accommodates approximately 53 photovoltaic modules, while the remaining approximately 167 modules are relocated to the auxiliary roofs of two adjacent buildings with the same orientation as the main roof.

Regarding the capital constraint of Equation (9): the total portfolio investment (45,000 + 12,328 = 57,328 USD) lies within the available budget, so the capital constraint holds with slack—it is inactive—and the linear program of Equation (9) degenerates exactly to the single-constraint greedy allocation by the marginal value applied above. Both constraints are retained in the framework formulation for generality; the present case demonstrates the single active constraint regime, in which the equivalence stated in Section 2.5 applies. A case in which capital, rather than area, is the binding constraint would follow the same procedure with $C_{\max}$ replacing A_{roof} as the exhausted resource.

3.4. Performance Indicators of the Portfolio

Once the portfolio is defined—solar thermal for DHW and photovoltaics for electricity, with annual solar fractions close to 100% in both vectors on an energy balance basis—its economic performance is evaluated. The photovoltaic system is assessed through a 25-year cash flow model with an annual revenue of 16,900 USD (displaced grid electricity), a 35% tax rate, straight-line depreciation of the investment over 10 years, and a real discount rate including a risk premium of 11.74%. The two discount rates used in this study serve different purposes: the nominal financing rate ($i = 16.35\%$) enters the capital recovery factor of the levelized cost comparison (Section 3.2), whereas the cash flow valuation adopts the real rate with risk premium (11.74%). The nominal rate is taken from the primary source, and the real rate is derived from its parameters through the Fisher relation, combining a 7% inflation rate and a 3% risk margin: $(1.1635/1.07 - 1) + 0.03 = 0.1174$. It should be noted, in addition, that the Level 2 selection is structurally insensitive to this choice: since O&M is proportional to the investment in both alternatives, Equation (3) implies $\psi = C_{\text{inv,ST}}/C_{\text{inv,PV-HP}}$ exactly, independent of the discount rate, the lifetime, and the O&M fraction.

Figure 8 shows the cumulative discounted cash flow over the system lifetime, while Table 8 summarizes the performance indicators.

Table 8. Performance indicators of the selected solar portfolio.

Indicator	Electrical Vector (PV)	Thermal Vector (ST)	Portfolio
Solar fraction (annual, energy balance)	≈100%	≈100%	—
Investment (USD)	45,000	12,328	57,328
Annual savings (USD)	16,900	11,429	28,329
NPV (USD)	55,327	—	—
IRR	≈28%	—	—
Payback (years)	≈5 (discounted)	≈1.1 (simple)	—
CO_2 avoided (t/year)	46.7	39.8	86.5

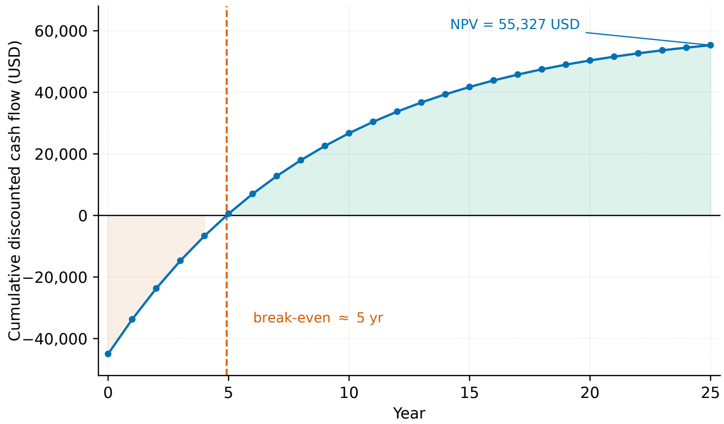

Figure 8. Economic projection of the photovoltaic system: cumulative discounted cash flow over the lifetime. Starting from an initial investment of 45,000 USD, the break-even point is reached at approximately 5 years (dashed line), with a net present value (NPV) of 55,327 USD at 25 years; the cash flow includes taxation (35%) and depreciation effects, discounted at a real rate with risk premium (11.74%).

The cash flow analysis starts from an initial investment of 45,000 USD, reaches the break-even point at approximately 5 years, and yields a net present value of 55,327 USD over the system lifetime, with an internal rate of return of approximately 28%. The solar thermal system, with annual savings of 11,429 USD against an investment of 12,328 USD, achieves a simple payback period of approximately 1.1 years. Overall, the portfolio saves 28,329 USD/year and avoids 86.5 t CO_2/year, equivalent to the total emissions of the baseline scenario.

An operational qualification is required for the electrical vector. The photovoltaic system includes no electrochemical storage, so the annual energy balance does not imply hour-by-hour self-sufficiency: generation is concentrated in the 10:30–15:30 window, whereas part of the demand (notably nighttime air conditioning) falls outside it. No net-metering or export remuneration scheme is assumed in the economic evaluation—revenues from surplus sales to the national grid during low-occupancy periods were explicitly excluded; a conservative choice—and the reported figure must therefore be read as an annual solar fraction on an energy balance basis, with the grid acting as the implicit buffer. The operational self-consumption fraction will necessarily be lower, and its quantification requires the hourly analysis identified as future research line (4). The thermal vector is not affected by this qualification to the same degree, since the DHW installation includes physical storage tanks that decouple solar collection from consumption.

A baseline projection is then carried out over the system lifetime to quantify the cumulative effect of substitution. Figure 9 compares, year by year, the cost (a) and emissions (b) of continuing with fossil-based supply versus those of the solar portfolio.

Over 25 years, the fossil baseline accumulates approximately 708,000 USD and 2162 t CO_2, whereas the solar portfolio accumulates approximately 86,000 USD and approximately 0 t of operational emissions (embodied life-cycle emissions from manufacturing and component replacement lie outside the accounting boundary [52]). The cumulative expenditures of both alternatives converge at approximately 2 years, after which the solar portfolio generates increasing savings reaching approximately 622,000 USD over the system lifetime.

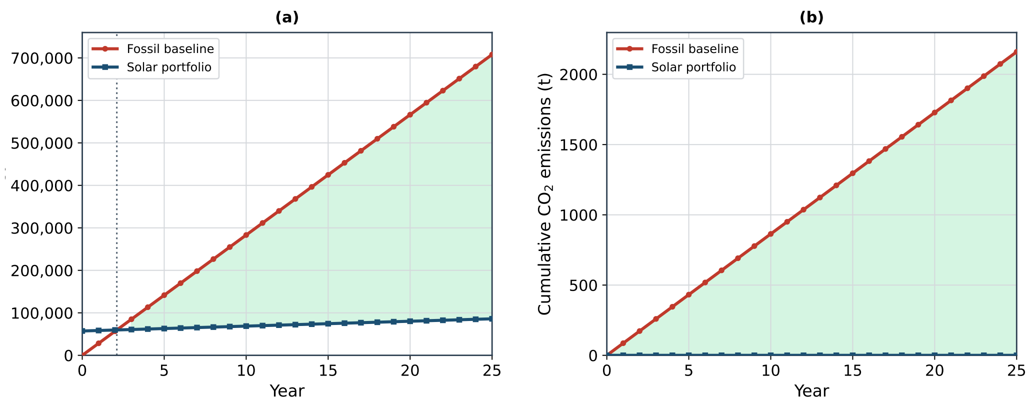

Figure 9. Baseline projection over the system lifetime. (**a**) Cumulative energy cost: the fossil baseline reaches approximately 708,000 USD over 25 years versus approximately 86,000 USD for the solar portfolio, with cost parity reached at approximately 2 years (dashed line). (**b**) Cumulative CO_2 emissions: approximately 2162 t for the baseline versus approximately 0 for the solar portfolio. The shaded area represents both economic savings and avoided emissions.

3.5. Sensitivity Analysis

Finally, the framework decisions are tested against uncertainty in the most sensitive parameters to verify that they do not depend on a single-point estimate. Figure 10 plots the ratio ψ as a function of the heat pump seasonal coefficient of performance (COP) (ranging from 2.5 to 4.5), for three unit cost levels (18,000, 36,000, and 54,000 USD).

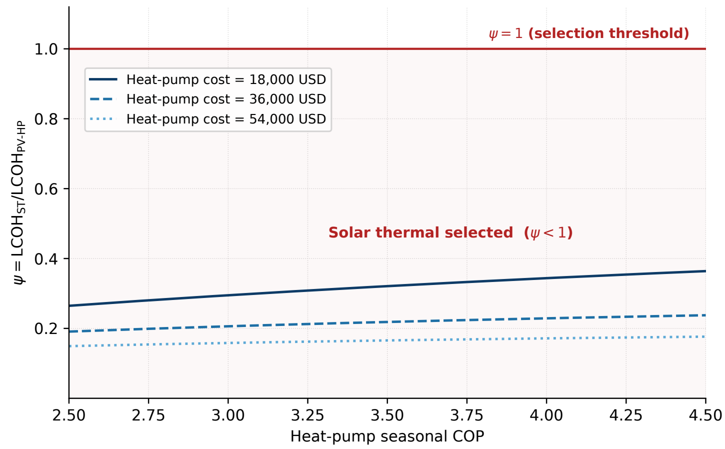

Figure 10. Sensitivity analysis of Level 2 selection. The ratio $\psi = \mathrm{LCOH_{ST}}/\mathrm{LCOH_{PV\text{-}HP}}$ remains below the threshold $\psi = 1$ across the full range of seasonal COP values and heat pump costs.

Across the explored domain, ψ remains between 0.15 and 0.37, always below the threshold $\psi = 1$ that would invert the selection: the choice of solar thermal is therefore not reversed. The roof allocation priority is also preserved under a 33% increase in collector footprint ($a_{\mathrm{ST}} = 6\ \mathrm{m}^2$, with $v_{th} \approx 83$ versus $v_{pv} \approx 32\ \mathrm{USD/m^2/year}$). Finally, avoided emissions scale linearly with the carbon intensity of the grid: under a conservative value of 400 g CO_2eq/kWh, the environmental benefit remains in the range of approximately 70–87 t CO_2/year.

The sensitivity domain is then extended to the full parameter set requested by the decision problem: Figure 11 subjects the three framework decisions (ψ, v_{th}/v_{pv}, and R_{TE}) to a tornado analysis under ±30% parameter variations, covering the investment costs, both energy prices, both specific yields and footprints, the distribution efficiency, and the estimated summer quarter.

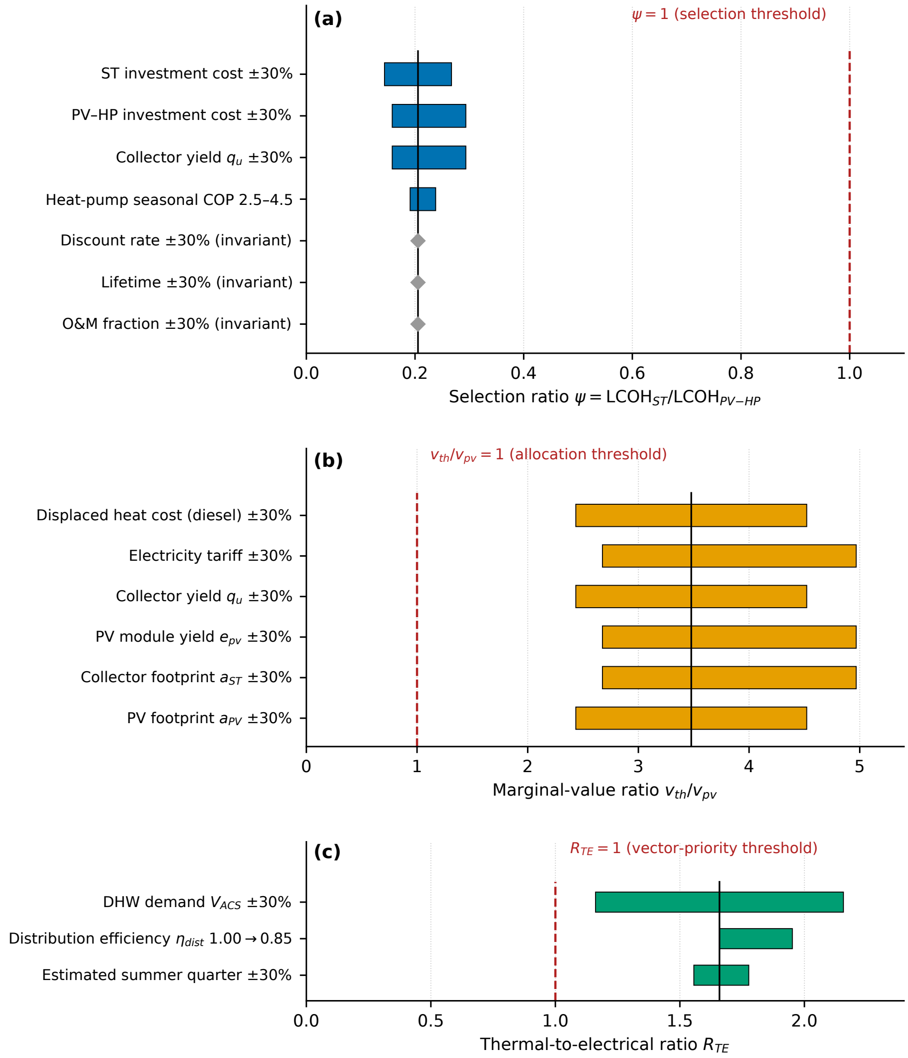

Figure 11. Extended tornado sensitivity analysis of the three framework decisions under ±30% parameter variations. (**a**) Selection ratio ψ: it never crosses the threshold $\psi = 1$ and is exactly invariant to the discount rate, the lifetime, and the O&M fraction (grey diamonds). (**b**) Marginal value ratio v_{th}/v_{pv}: it remains between 2.4 and 5.0. (**c**) Thermal-to-electrical ratio R_{TE}: it remains between 1.16 and 2.16, including a distribution efficiency of $\eta_{dist} = 0.85$ and a ±30% error in the estimated summer quarter. Vertical solid lines indicate baseline values; dashed lines indicate decision thresholds.

Panel (a) of Figure 11 shows that ψ remains within 0.14–0.29 under ±30% variations of the ST investment cost, the PV-HP investment cost, and the collector yield, and within 0.19–0.24 across the seasonal COP range 2.5–4.5; it is, moreover, exactly invariant to the discount rate, the lifetime, and the O&M fraction, since these terms cancel in the ratio when O&M is proportional to investment. Panel (b) shows that the marginal value ratio v_{th}/v_{pv} remains within 2.4–5.0 under ±30% variations of the displaced diesel price, the electricity tariff, both specific yields (q_u, e_{pv}), and both footprints (a_{ST}, a_{PV}). Panel (c) shows that R_{TE} remains within 1.16–2.16 under a ±30% variation of the DHW demand, a distribution efficiency reduced to $\eta_{dist} = 0.85$ (which raises E_{th} to approximately 149,900 $\mathrm{kWh_{th}}$/year and R_{TE} to 1.95), and a ±30% error in the proportionally estimated summer quarter ($E_{el} \in [71{,}732, 81{,}904]$ kWh/year). None of the three decision thresholds ($\psi = 1$, $v_{th}/v_{pv} = 1$, $R_{TE} = 1$) is crossed at any point of the explored domain: all three framework decisions are ordinally robust. In particular, the assumption $\eta_{dist} = 1$ is conservative with respect to the thermal-priority decision, since any realistic loss level increases the weight of the thermal vector, while ψ is unaffected because both thermal alternatives deliver the same useful heat Q_u.

The economic indicators were also stress-tested. The simple payback of the solar thermal system ranges from 0.83 to 1.54 years under a $\pm 30\%$ variation of the diesel price, and does not exceed 2.0 years even under the joint adverse case (investment $+30\%$ and savings -30% simultaneously). For the photovoltaic system, the internal rate of return (28%) more than doubles the discount rate (11.74%), so the net present value remains strictly positive under a 30% reduction of the electricity tariff. The short payback periods are thus a structural consequence of the local price context—displaced electricity at 0.22 USD/kWh and diesel at 0.77 USD/L against low local capital costs—rather than an artifact of optimistic assumptions.

4. Discussion

The audit identified air conditioning as the significant energy use, accounting for 77% of the connected load, consistent with evidence that in warm-climate hospitality buildings, cooling systems are the dominant electricity consumers and the main contributors to operational footprint [54]; a similar pattern has been reported for university campuses in hot climates, where air conditioning can reach 79% of the electrical load [13]. However, the key finding emerges when demand is disaggregated by energy vector: the domestic hot water thermal demand, 127,440 kWh_{th}/year, exceeds total electrical demand, 76,818 kWh/year, yielding a thermal-to-electrical ratio of $R_{TE} = 1.66$.

The most visible load in terms of installed power—air conditioning—does not coincide with the dominant energy vector—thermal demand—because hot water production (8700 L/day for 75 beds) operates almost continuously, whereas the electrical system operates for only approximately 668 equivalent full-load hours. This decoupling between installed power and annual energy demand is precisely why a load-based sizing approach would misidentify the priority vector, and it justifies the use of an audit-based characterization of consumption—the standard approach in hospitality energy assessments [54]—rather than generic end-use allocations.

The baseline indicators obtained (specific cost of 378 USD/(bed·year) and specific emissions of 1153 kg CO_2/(bed·year)) are consistent with energy, emissions, and cost intensity metrics commonly used to benchmark tropical hotels based on audit data [55].

For the thermal vector, the framework selects solar thermal over photovoltaic with heat pump, with levelized heat costs of 0.018 and 0.088 USD/kWh_{th}, respectively ($\psi = 0.21$). These values are significantly lower than European benchmarks—Nielsen et al. report 0.23 EUR/kWh for a solar thermal hot water system and 0.34 EUR/kWh for a photovoltaic-based system with heat pump [56]—a difference attributable to lower local investment costs: the solar thermal LCOH is dominated (89%) by capital expenditure, and the evacuated tube collectors used, locally assembled at 536 USD each, substantially reduce this capital component.

That the levelized cost is governed by investment implies that the decision is highly sensitive to manufacturing costs, giving local production a decisive role. The advantage of solar thermal also has a physical basis: it converts solar radiation directly into heat (approximately 70–90% efficiency), whereas the photovoltaic pathway involves two conversion stages—first to electricity (18–20% efficiency), and then to heat via the heat pump—resulting in a useful heat yield of approximately $\sim$1230 $kWh_{th}/(m^2 \cdot year)$ for the collector versus $\sim$145 $kWh_{el}/(m^2 \cdot year)$ for the PV module.

The literature, however, is not unanimous. El Mardi et al. find the photovoltaic heat pump option more favorable for a swimming pool application in Morocco (levelized cost of 0.026 USD/kWh and a payback period of 4.4 years), identifying the coefficient of performance, diesel cost, and collector/panel cost as the critical parameters [57]—precisely the variables that drive ψ. The selection is therefore context-dependent; in this case, low investment costs and prevailing energy prices keep ψ well below unity.

The allocation between vectors is resolved through the marginal value per unit of surface: $v_{th} \approx 111$ versus $v_{pv} \approx 32$ USD/(m^2·year), a ratio of 3.5 in favor of solar thermal. It is useful to clarify the origin of this ratio, since $v = y \cdot c$ is the product of specific yield and the unit value of displaced energy: although the unit value favors electricity ($c_{th}/c_{el} \approx 0.41$), the yield advantage per unit area of the collector ($y_{th}/y_{el} \approx 8.5$) dominates it by a wide margin.

Under the roof constraint (237 m^2), the criterion assigns first 104 m^2 to the 23 collectors—enough to satisfy the thermal demand—and allocates the remaining surface (134 m^2) to 53 photovoltaic modules. This rule, equivalent to saturating the technology with the highest marginal value before moving to the next, is the solution of the allocation problem under a single active constraint: v_i acts as the shadow price of roof area for each technology, and maximizing annual value requires prioritizing the highest one.

This criterion corrects the original project layout, which prioritized photovoltaic deployment on the main roof, and is consistent with evidence showing that photovoltaic systems require roughly three times more surface area than solar thermal systems for equivalent hot water coverage [56], as well as with integrated planning frameworks where combined thermal and electrical systems under area constraints show that the optimal mix is highly dependent on local electricity prices [58].

From an economic perspective, the photovoltaic system yields a net present value of 55,327 USD, a discounted payback period of approximately 5 years, and an internal rate of return of 28%, while the solar thermal system pays back in 1.1 years (investment of 12,328 USD versus annual savings of 11,429 USD). These short payback periods reflect the high value of displaced energy in the local context—electricity at 0.22 USD/kWh and diesel at 0.77 USD/L. As shown in Section 3.5, these indicators degrade gracefully rather than collapse under adverse assumptions: the ST payback stays below 2.0 years even when investment rises 30% and savings fall 30% simultaneously, and the PV net present value remains positive under a 30% tariff reduction.

The photovoltaic payback period is of the same order as the 4.4 years reported for photovoltaic heat pump systems in [57], while the notably faster payback of solar thermal is driven by its low capital cost and the high diesel price it displaces. It should be explicitly noted that these absolute values are context-specific to the case study price structure (with a 1:1 Cuban convertible peso–USD parity assumed from the primary source): what is transferable is the decision logic, which is relative to prices, rather than the specific monetary magnitudes.

Both interventions jointly avoid 86.5 t CO_2/year (46.7 from the electrical vector and 39.8 from the thermal vector), reaching an annual solar fraction close to 100% in both vectors on an energy balance basis. Over a 25-year horizon, this corresponds to approximately 2162 t CO_2 avoided. The near-unity solar fraction is characteristic of sites with abundant solar irradiation, consistent with full solar fraction regimes reported for thermal applications under high-irradiance conditions [58]; for the electrical vector, however, this figure describes the annual balance and not the hour-by-hour operational coverage, as qualified in Section 3.4.

However, environmental performance is highly sensitive to the grid emission factor: when it is varied between 400 and 608 g CO_2/kWh, avoided emissions range from 70 to 87 t/year. This sensitivity helps explain why El Mardi et al. report that photovoltaic systems with heat pumps may avoid less CO_2 than solar thermal systems in their specific context [57]: the environmental benefit depends strongly on the carbon intensity of the displaced electricity, which in the Cuban case is high (608 g CO_2/kWh) and favors both photovoltaics and, through diesel substitution, solar thermal systems.

From a methodological standpoint, the value of the framework lies in chaining diagnosis, selection, and allocation in a deterministic manner, replacing the subjective weighting schemes of multi-criteria methods—commonly used in renewable energy technology selection [59]—with observable economic criteria. In AHP- or TOPSIS-type methods, the ranking of alternatives depends on decision-maker-assigned weights, whose influence is a well-known limitation that has motivated the development of objective weighting schemes [25].

Here, by contrast, intravector selection is governed by the levelized cost of heat and intervector allocation by marginal value—both verifiable quantities that make the decision reproducible by third parties. The framework is also distinct from ex post evaluations (3E, exergy, or life-cycle assessment) of a pre-defined configuration, in that it prescribes the configuration directly from the diagnostic stage rather than merely assessing its performance.

4.1. Comparison with the Literature

To position the scope and novelty of the framework, it is useful to contrast it with the literature on evaluation, sizing, and selection of solar technologies in buildings. Table 9 compiles eighteen studies—the present work and seventeen previous contributions—and characterizes them along five dimensions: system and location, decision approach, selected technology, key reported indicator, and methodological feature.

The selected studies cover both the relevant technological space—domestic hot water via solar thermal, photovoltaic systems, photovoltaic–thermal (PVT) systems and PVT with heat pumps, swimming pool heating, district heating networks, and life-cycle assessment—as well as the two dominant methodological families: techno-economic evaluation of a predefined system and multi-criteria decision-making for plant siting.

The purpose of the comparison is not to rank performance—which is not comparable across climates, price structures, and demand profiles—but to contrast *what* is being decided and *how* the decision is made.

Table 9. Position of the present study with respect to the literature on the assessment, sizing, and selection of solar technologies in buildings.

Study	System/Location	Decision Approach	Technology	Key Indicator and Distinctive Feature
This study	University residence hall, Cienfuegos (Cuba)	Three-level deterministic framework by energy vector (LCOH + marginal value)	Solar thermal (DHW) + photovoltaic (electricity)	$\psi = 0.21$; $LCOH_{ST} = 0.018$ USD/kWh_{th}; PV: NPV = 55,327 USD, IRR = 28%, discounted PBP ≈ 5 yr; ST simple PBP 1.1 yr; allocation under roof-area constraint by marginal value
[56]	DHW: PV vs. solar thermal, Denmark	Experimental assessment and simulation	Solar thermal	LCoH 0.23 (ST) vs. 0.34 (PV) EUR/kWh; PV requires ≈ 3× more area
[52]	DHW, domestic scale (Italy)	Life-cycle assessment (LCA)	PV and solar thermal	Compares environmental footprint of PV (silicon, thin-film) vs. solar thermal
[22]	DHW, cold climate (Canada)	Simulation (TRNSYS), four systems	PVT + heat pump	Annual solar fraction 76.7%; superior winter performance vs. conventional solar thermal
[23]	DHW, multifamily building (Europe)	Validated simulation	Glazed PVT	Thermal yield 352–582 and electrical yield 63–149 kWh m^{-2} yr^{-1}
[57]	Indoor swimming pool, Fez (Morocco)	Techno-economic comparison (3 configurations)	PV + heat pump	LCOH 0.026 USD/kWh; PBP 4.4 yr; COP, diesel and collector cost are key drivers
[60]	University swimming pool, Naples (Italy)	Dynamic simulation + experiment	Evacuated-tube solar thermal	Best energy-economic performance; PBP 14 yr (no incentive), 5 yr (with incentives)
[20]	DHW + electricity, dwelling (UK)	Techno-economic analysis	PVT + heat pump	Covers ∼80% DHW and ∼30% electricity; discounted PBP 14 yr

Table 9. *Cont.*

Study	System/Location	Decision Approach	Technology	Key Indicator and Distinctive Feature
[61]	Cooling, heating, power; tropical climate	Performance + economic assessment	Cascade PVT + heat pump	Polygeneration (CCHP) for tropical climate applications
[62]	Residential building (Italy)	Dynamic simulation + thermoeconomic optimization	Heat pump driven by PVT collectors	Thermoeconomic optimization of integrated PVT–heat pump system
[63]	DHW, dwelling (Krakow, Poland)	One-year operational monitoring	PV + air-source heat pump	Increases PV self-consumption
[64]	Space conditioning + DHW, dwelling (Italy)	Simulation with rule-based control	PV + modulating heat pump	Control strategy to maximize PV self-consumption
[58]	Solar district heating; Athens, Munich, Copenhagen	Unified techno-economic sizing under area constraint	Context-dependent mix	100% solar fraction (Athens); optimal mix depends on electricity price
[59]	Power systems (systematic review)	Multi-criteria decision-making (TOPSIS) with weighting	— (review)	Highlights subjectivity of weights in MCDM approaches
[25]	PV-plant siting, Saudi Arabia	CRITIC–TOPSIS (objective weights)	Optimal site selection	Reduces AHP subjectivity using CRITIC-derived weights
[26]	PV-plant siting, Saudi Arabia	GIS–AHP	Optimal PV site	Land suitability mapping with sensitivity analysis
[27]	PV-plant siting, Malatya (Turkey)	GIS–AHP	Optimal PV site	GIS-based suitability assessment using AHP
[28]	PV-plant siting, Iran	Risk-based multi-criteria spatial analysis	Optimal PV site	Integrates risk into spatial decision framework

The joint reading of Table 9 shows, first, that the literature does not converge toward a single optimal solar technology for buildings: its conclusions are strongly context-dependent. For domestic hot water applications, one group of studies favors solar thermal systems due to their lower levelized cost and smaller surface requirements—Nielsen et al. report that photovoltaics require roughly three times more area for equivalent coverage [56], and evacuated-tube solar thermal systems are identified as the most suitable option in swimming pool retrofits [60]—in agreement with the selection obtained in this work.

A second group favors the electrical pathway: photovoltaic systems coupled with heat pumps become preferable under different climatic conditions and price structures [57], while photovoltaic–aerothermal systems maximize self-consumption in temperate latitudes [63]. A third group supports photovoltaic–thermal hybrid configurations, with or without heat pumps, due to their higher combined thermal and electrical output per unit area [20,22,23,61,62,64].

This dispersion does not indicate a contradiction in the literature; rather, it reveals that the outcome is governed by a limited set of parameters—electricity price, displaced fuel cost, coefficient of performance, investment cost, and solar resource availability. The ratio ψ proposed here makes this dependency explicit and, when evaluated in the present case context, remains well below unity, placing the solar thermal selection in the same regime as [56,60], and clearly separating it from cases such as [57].

Consistently, the levelized costs obtained here are lower than European values [56] due to reduced local investment costs, and the thermal yields per unit area reported for PVT collectors (352–582 kWh/(m^2·year) [23]) confirm the order of magnitude used in the marginal value analysis.

From a methodological standpoint, the contrast is even more pronounced. Techno-economic studies [20,22,23,52,56–58,60–64] evaluate or size a pre-defined system: they answer how much a given configuration costs and how much energy it delivers, but not which configuration should be chosen nor how a scarce surface should be allocated among competing energy vectors.

Multi-criteria studies [25–28,59] do make decisions, but they are predominantly focused on large-scale photovoltaic plant siting and rely on weighting schemes—AHP, TOPSIS, GIS-based approaches—whose parameters are ultimately set by expert judgment. The literature itself acknowledges this subjectivity as a limitation and has developed objective weighting schemes such as CRITIC or entropy methods to mitigate it [25].

The framework proposed here occupies a space not covered by either family: it makes decisions like multi-criteria methods, but at building scale and explicitly by energy vector, and it does so, unlike them, using observable economic criteria without subjective weights. It chains diagnosis, intravector selection via levelized cost, and intervector allocation via marginal value into a single deterministic and auditable procedure. In contrast to ex post assessments—3E, exergetic, or life-cycle analyses [52]—which evaluate a pre-selected configuration, the proposed framework prescribes the configuration directly from the diagnostic stage.

This combination—vector-based decision-making, observable economic criteria, and full traceability—is, within the limits of the comparison in Table 9, what distinguishes the present work.

4.2. Study Limitations

It is important to clearly delimit the scope of the results, distinguishing internal validity from external validity:

(i) Single case study. This work constitutes a demonstration of the proposed framework rather than a statistical validation across building typologies. What is generalizable is the decision-making logic, not the numerical results of the case study; its transferability to other building types and climates remains an open question of external validity.

(ii) Most uncertain input parameter. The unit cost of the heat pump is a market-derived parameter subject to variability. However, it is important to distinguish between ordinal robustness and cardinal precision: the sensitivity analysis shows that ψ remains well below unity across the entire range of coefficient of performance and cost values tested, so that the *selection* of solar thermal technology does not change even if the exact levelized cost value is uncertain.

(iii) Collector footprint. The unit surface area of the collector used in the marginal value rule is an estimated geometric parameter. Nevertheless, the priority of roof allocation remains unchanged even when this footprint is increased by 33%, reinforcing the stability of the intervector decision.

(iv) Deterministic nature of the approach. As a single-case study, the analysis does not include statistical inference. Robustness is assessed through sensitivity analysis; stochastic uncertainty propagation would quantify confidence in probabilistic terms, but would not alter the ordinal conclusions of the model.

(v) Dependence on price context. The economic results reflect the price structure of the case study (parity of 1 Cuban convertible peso = 1 USD as assumed in the primary source). Therefore, absolute values are context-specific, while the relative decision logic based on price ratios remains transferable.

(vi) Bounded technology set. The framework ranks alternatives only within the considered set (solar thermal, photovoltaic, and photovoltaic with heat pump). It does not explore technologies outside this predefined space.

(vii) Annual energy balance basis and data vintage. All solar fractions are computed on an annual energy balance, without hourly resolution or storage modeling for the electrical vector; the operational self-consumption fraction will be lower than the annual figure, and no export remuneration was assumed. In addition, the meter readings correspond to 2016–2017 (the last complete pre-disruption series) and the missing summer quarter was estimated proportionally; the sensitivity analysis shows that a $\pm 30\%$ error in this estimate does not alter any framework decision. Both aspects motivate future research line (4).

4.3. Future Research Directions

Building on the limitations identified above, four priority research lines are identified:

(1) Transferability. Apply the protocol to other building typologies and climates, with different price structures and resource conditions, in order to verify that the diagnosis–selection–allocation chain retains its discriminative power and to delineate the validity domain of each decision rule.
(2) Probabilistic layer. Couple the framework with a Monte Carlo-type uncertainty propagation, using justified input distributions, to report confidence intervals for ψ as well as for marginal values, and to quantify the probability of inversion of each decision.
(3) Technology expansion. Include additional technologies—in particular photovoltaic–thermal (PVT) collectors, which co-produce both energy vectors from the same surface—which would require generalizing the marginal value rule to the case of joint products and possibly reformulating the ψ boundary condition.
(4) Temporal resolution. Replace the annual energy formulation with hourly demand and solar resource profiles, so that temporal matching between generation and consumption, and consequently storage sizing, are explicitly included in both the selection and allocation stages.

5. Conclusions

This study formalized the energy audit within a three-level deterministic decision-making framework that selects and sizes solar technologies in buildings by energy vector, and demonstrated it in a university residence in Cienfuegos, Cuba. The audit revealed that the most visible load in terms of installed power—air conditioning, which accounts for 77% of the connected demand and constitutes the significant energy use—does not coincide with the dominant vector in terms of annual energy. When the demand is disaggregated by vector, the thermal requirement for domestic hot water (127,440 kWh_{th}/year) exceeds the entire electrical demand (76,818 kWh/year), yielding a thermal-to-electric ratio of $R_{\text{TE}} = 1.66$. This decoupling between installed power and annual energy is the central result that justifies allocating the solar portfolio by energy vector rather than by connected load.

At the second level, the levelized cost of heat selects solar thermal over the photovoltaic with heat pump pathway for the thermal vector (0.018 vs. 0.088 USD/kWh_{th}; selection ratio $\psi = 0.21$); this hierarchy is robust, since ψ remains well below unity across the full range of heat pump coefficient of performance and cost values tested, and is exactly invariant to the discount rate, the lifetime, and the O&M fraction. At the third level, marginal value per unit of surface governs the allocation between vectors: $v_{\text{th}} \approx 111$ vs. $v_{\text{pv}} \approx 32$ USD/(m^2·year), a ratio of 3.5 in favor of solar thermal. Under the roof constraint of 237 m^2, the criterion assigns 104 m^2 to 23 thermal collectors and the remaining 134 m^2 to 53 photovoltaic modules, reversing the original design, which had allocated the main roof area to photovoltaics. The photovoltaic sizing decision is robust to the statistical design criterion: the deployed, area-bounded fleet of 220 modules covers 104.5% of the annual demand, only 4.3% above the annual mean sizing, and with nine monthly readings, the empirical P90 coincides in practice with the design maximum.

In economic terms, the photovoltaic subsystem yields a net present value of USD 55,327, a discounted payback of approximately 5 years, and an internal rate of return of 28%, whereas the solar thermal subsystem recovers its investment in 1.1 years, due to its low capital cost and the high price of displaced diesel. Overall, both interventions achieve an annual solar fraction close to 100% in both vectors on an energy balance basis (the hour-by-hour operational self-consumption of the electrical vector will be lower in the absence of storage) and avoid 86.5 t CO_2/year of operational emissions (46.7 from the electrical vector and 39.8 from the thermal one), equivalent to approximately 2162 t CO_2 over a 25-year horizon; this value remains between 70 and 87 t/year when the grid emission factor varies between 400 and 608 g CO_2/kWh. Relative to the baseline energy performance indicators—a specific cost of 378 USD/(bed·year), specific emissions of 1153 kg CO_2/(bed·year), and an energy intensity of 2723 kWh/(bed·year)—these results quantify the benefit of the vector-based solar portfolio.

From a methodological perspective, the framework chains diagnosis, selection, and allocation into a single auditable procedure that replaces the subjective expert weights of conventional multi-criteria methods with observable economic criteria, and that operates at the building scale and by energy vector—a niche not covered either by techno-economic studies, which evaluate a fixed system, or by multi-criteria approaches, which rank large-scale plant locations. Since each decision is based on ratios linked to local prices, the transferable contribution lies in the decision logic rather than in the absolute monetary values, which are specific to the price context of the case study. This work constitutes a single-case demonstration and not a statistical validation; consequently, future research should test the protocol across different building typologies and climates, incorporate a probabilistic layer to propagate input uncertainty into ψ and marginal values, expand the technology set to include photovoltaic–thermal (PVT) collectors that co-produce both vectors, and move from annual energy balances to hourly resolution so that temporal matching between generation and demand—and thus storage sizing—is explicitly embedded in the selection process.

Author Contributions: Conceptualization, H.N.K. and Y.C.A.; methodology, R.J.B. and Y.C.A.; software, L.A.I.C., S.T., M.G.-A. and R.J.B. ; validation, J.P.M.Y., J.R.G.S. and J.R.-R.; formal analysis, L.A.I.C., S.T., H.N.K. and R.J.B.; investigation, H.N.K., M.G.-A., R.J.B. and Y.C.A.; resources, J.R.G.S. and Y.C.A.; data curation, L.A.I.C., R.J.B., M.G.-A. and J.R.-R.; writing—original draft preparation, H.N.K.,Y.C.A. and R.J.B.; writing—review and editing, J.P.M.Y., M.G.-A., J.R.G.S., R.J.B., L.A.I.C. and J.R.-R.; visualization, H.N.K.; supervision, Y.C.A. and J.R.-R.; project administration, Y.C.A. All authors have read and agreed to the published version of the manuscript.

Funding: This research received no external funding.

Institutional Review Board Statement: Not applicable.

Informed Consent Statement: Not applicable.

Data Availability Statement: The original contributions presented in this study are included in the article. Further inquiries may be directed to the corresponding authors.

Acknowledgments: The authors have reviewed and edited the output and take full responsibility for the content of this publication.

Conflicts of Interest: The authors declare no conflicts of interest.

Abbreviations

The following abbreviations are used in this manuscript:

AHP	Analytic Hierarchy Process
BIPV	Building-Integrated Photovoltaics
COP	Coefficient of Performance
CRF	Capital Recovery Factor
CRITIC	Criteria Importance Through Intercriteria Correlation
DHW	Domestic Hot Water
EnPI	Energy Performance Indicator
GIS	Geographic Information System
HSP	Peak Sun Hours
IRR	Internal Rate of Return
LCA	Life-Cycle Assessment
LCOH	Levelized Cost of Heat
MCDM	Multi-Criteria Decision-Making
NPV	Net Present Value
PBP	Payback Period
PR	Performance Ratio
PV	Photovoltaic
PV-HP	Photovoltaic Coupled to a Heat Pump
PVT	Photovoltaic–Thermal
R_{TE}	Thermal-to-Electric Ratio
SF	Solar Fraction
ST	Solar Thermal
TOPSIS	Technique for Order of Preference by Similarity to Ideal Solution

References

1. United Nations Environment Programme; Global Alliance for Buildings and Construction. Global Status Report for Buildings and Construction 2024/2025: Not Just Another Brick in the Wall. 2025. Available online: https://www.unep.org/resources/report/global-status-report-buildings-and-construction-20242025 (accessed on 21 July 2026).
2. Iweh, C.D.; Gyamfi, S.; Tanyi, E.; Effah-Donyina, E. Distributed Generation and Renewable Energy Integration into the Grid: Prerequisites, Push Factors, Practical Options, Issues and Merits. *Energies* **2021**, *14*, 5375. [CrossRef]
3. Brownsword, R.; Fleming, P.; Powell, J.; Pearsall, N. Sustainable Cities—Modelling Urban Energy Supply and Demand. *Appl. Energy* **2005**, *82*, 167–180. [CrossRef]
4. Bosu, I.; Mahmoud, H.; Ookawara, S.; Hassan, H. Applied Single and Hybrid Solar Energy Techniques for Building Energy Consumption and Thermal Comfort: A Comprehensive Review. *Sol. Energy* **2023**, *259*, 188–228. [CrossRef]
5. Blechinger, P.; Cader, C.; Bertheau, P.; Huyskens, H.; Seguin, R.; Breyer, C. Global Analysis of the Techno-Economic Potential of Renewable Energy Hybrid Systems on Small Islands. *Energy Policy* **2016**, *98*, 674–687. [CrossRef]
6. Wolf, F.; Surroop, D.; Singh, A.; Leal, W. Energy Access and Security Strategies in Small Island Developing States. *Energy Policy* **2016**, *98*, 663–673. [CrossRef]
7. Surroop, D.; Raghoo, P.; Wolf, F.; Shah, K.U.; Jeetah, P. Energy Access in Small Island Developing States: Status, Barriers and Policy Measures. *Environ. Dev.* **2018**, *27*, 58–69. [CrossRef]
8. Shono, K.; Yamaguchi, Y.; Perwez, U.; Ma, T.; Dai, Y.; Shimoda, Y. Large-Scale Building-Integrated Photovoltaics Installation on Building Façades: Hourly Resolution Analysis Using Commercial Building Stock in Tokyo, Japan. *Sol. Energy* **2023**, *253*, 137–153. [CrossRef]
9. Talwar, P.; Verma, N.; Khatri, H.; Ahire, P.D.; Chaudhary, G.; Lindenberger, C.; Vivekanand, V. A Systematic Review of Photovoltaic-Green Roof Systems in Different Climatic Conditions Focusing on Sustainable Cities and Societies. *Sustain. Cities Soc.* **2023**, *98*, 104813. [CrossRef]
10. Wijeratne, W.P.U.; Yang, R.J.; Too, E.; Wakefield, R. Design and Development of Distributed Solar PV Systems: Do the Current Tools Work? *Sustain. Cities Soc.* **2019**, *45*, 553–578. [CrossRef]
11. Ahmed, A.; Nadeem, T.B.; Naqvi, A.A.; Siddiqui, M.A.; Khan, M.H.; Bin Zahid, M.S.; Ammar, S.M. Investigation of PV Utilizability on University Buildings: A Case Study of Karachi, Pakistan. *Renew. Energy* **2022**, *195*, 238–251. [CrossRef]

12. Ouhammou, B.; Gargab, F.Z.; El Idrissi Kaitouni, S.; Smouh, S.; El Mrabet, R.; Aggour, M.; Jamil, A.; Kousksou, T. Energy Saving Potential Diagnosis for Moroccan University Campuses. *AIMS Energy* **2023**, *11*, 576–611. [CrossRef]
13. Alsulamy, S.; Bahaj, A.S.; James, P.; Alghamdi, N. Solar PV Penetration Scenarios for a University Campus in KSA. *Energies* **2022**, *15*, 3150. [CrossRef]
14. Hurtado-Pérez, E.; Bastida-Molina, P.; Aparisi-Cerdá, I.; Alfonso-Solar, D.; Fernández, A.R. Multicriteria Solar Photovoltaic Potential Evaluation for High Educational Buildings. Case Study of Polytechnic University of Valencia, Spain. *Renew. Energy* **2024**, *227*, 120560. [CrossRef]
15. Sterling, S.; Collins, M. Feasibility Analysis of an Indirect Heat Pump Assisted Solar Domestic Hot Water System. *Appl. Energy* **2012**, *93*, 11–17. [CrossRef]
16. Bosu, I.; Mahmoud, H.; Hassan, H. Energy Audit, Techno-Economic, and Environmental Assessment of Integrating Solar Technologies for Energy Management in a University Residential Building: A Case Study. *Appl. Energy* **2023**, *341*, 121141. [CrossRef]
17. Buker, M.S.; Riffat, S.B. Solar Assisted Heat Pump Systems for Low Temperature Water Heating Applications: A Systematic Review. *Renew. Sustain. Energy Rev.* **2016**, *55*, 399–413. [CrossRef]
18. Mohanraj, M.; Belyayev, Y.; Jayaraj, S.; Kaltayev, A. Research and Developments on Solar Assisted Compression Heat Pump Systems—A Comprehensive Review (Part A: Modeling and Modifications). *Renew. Sustain. Energy Rev.* **2018**, *83*, 90–123. [CrossRef]
19. Moreno-Rodríguez, A.; González-Gil, A.; Izquierdo, M.; Garcia-Hernando, N. Theoretical Model and Experimental Validation of a Direct-Expansion Solar Assisted Heat Pump for Domestic Hot Water Applications. *Energy* **2012**, *45*, 704–715. [CrossRef]
20. Obalanlege, M.A.; Xu, J.; Markides, C.N.; Mahmoudi, Y. Techno-Economic Analysis of a Hybrid Photovoltaic-Thermal Solar-Assisted Heat Pump System for Domestic Hot Water and Power Generation. *Renew. Energy* **2022**, *196*, 720–736. [CrossRef]
21. Fine, J.; Friedman, J.; Dworkin, S. Detailed Modeling of a Novel Photovoltaic Thermal Cascade Heat Pump Domestic Water Heating System. *Renew. Energy* **2017**, *101*, 500–513. [CrossRef]
22. Emamjome Kashan, M.; Fung, A.S.; Swift, J. Integrating novel microchannel-based solar collectors with a water-to-water heat pump for cold-climate domestic hot water supply, including related solar systems comparisons. *Energies* **2021**, *14*, 4057. [CrossRef]
23. Pokorny, N.; Matuška, T. Glazed photovoltaic-thermal (PVT) collectors for domestic hot water preparation in multifamily building. *Sustainability* **2020**, *12*, 6071. [CrossRef]
24. Del Amo, A.; Martínez-Gracia, A.; Bayod-Rújula, A.A.; Cañada, M. Performance Analysis and Experimental Validation of a Solar-Assisted Heat Pump Fed by Photovoltaic-Thermal Collectors. *Energy* **2019**, *169*, 1214–1223. [CrossRef]
25. Hassan, I.; Alhamrouni, I.; Azhan, N.H. A CRITIC–TOPSIS Multi-Criteria Decision-Making Approach for Optimum Site Selection for Solar PV Farm. *Energies* **2023**, *16*, 4245. [CrossRef]
26. Al Garni, H.Z.; Awasthi, A. Solar PV power plant site selection using a GIS-AHP based approach with application in Saudi Arabia. *Appl. Energy* **2017**, *206*, 1225–1240. [CrossRef]
27. Colak, H.I.; Memisoglu, T.; Gercek, Y. Optimal site selection for solar photovoltaic (PV) power plants using GIS and AHP: A case study of Malatya Province, Turkey. *Renew. Energy* **2020**, *149*, 565–576. [CrossRef]
28. Shorabeh, S.N.; Firozjaei, M.K.; Nematollahi, O.; Firozjaei, H.K.; Jelokhani-Niaraki, M. A risk-based multi-criteria spatial decision analysis for solar power plant site selection in different climates: A case study in Iran. *Renew. Energy* **2019**, *143*, 958–973. [CrossRef]
29. El-Bayeh, C.Z.; Alzaareer, K.; Brahmi, B.; Zellagui, M.; Eicker, U. An Original Multi-Criteria Decision-Making Algorithm for Solar Panels Selection in Buildings. *Energy* **2021**, *217*, 119396. [CrossRef]
30. Gholami, H. A Holistic Multi-Criteria Assessment of Solar Energy Utilization on Urban Surfaces. *Energies* **2024**, *17*, 5328. [CrossRef]
31. Kurdi, Y.; Alkhatatbeh, B.J.; Asadi, S.; Jebelli, H. A Decision-Making Design Framework for the Integration of PV Systems in the Urban Energy Planning Process. *Renew. Energy* **2022**, *197*, 288–304. [CrossRef]
32. *ISO 50001:2018*; Energy Management Systems—Requirements with Guidance for Use. International Organization for Standardization: Geneva, Switzerland, 2018.
33. Bosu, I.; Mahmoud, H.; Hassan, H. Energy Audit and Management of an Industrial Site Based on Energy Efficiency, Economic, and Environmental Analysis. *Appl. Energy* **2023**, *333*, 120619. [CrossRef]
34. Sommerfeldt, N.; Madani, H. Revisiting the Techno-Economic Analysis Process for Building-Mounted, Grid-Connected Solar Photovoltaic Systems: Part One—Review. *Renew. Sustain. Energy Rev.* **2017**, *74*, 1379–1393. [CrossRef]
35. Poppi, S.; Sommerfeldt, N.; Bales, C.; Madani, H.; Lundqvist, P. Techno-Economic Review of Solar Heat Pump Systems for Residential Heating Applications. *Renew. Sustain. Energy Rev.* **2018**, *81*, 22–32. [CrossRef]
36. Mohanraj, M.; Belyayev, Y.; Jayaraj, S.; Kaltayev, A. Research and Developments on Solar Assisted Compression Heat Pump Systems—A Comprehensive Review (Part B: Applications). *Renew. Sustain. Energy Rev.* **2018**, *83*, 124–155. [CrossRef]

37. Vázquez, L.; Majanne, Y.; Castro, M.; Luukkanen, J.; Hohmeyer, O.; Vilaragut, M.; Díaz, D. Energy System Planning towards Renewable Power System: Energy Matrix Change in Cuba by 2030. *IFAC-PapersOnLine* **2018**, *51*, 522–527. [CrossRef]
38. Guevara-Luna, M.A.; Madrazo, J.; Meneses, E.; Mora, H.; Clappier, A. Strategies toward an Effective and Sustainable Energy Transition for Cuba. *Renew. Sustain. Energy Rev.* **2024**, *197*, 114387. [CrossRef]
39. Brandts, M.; Bertheau, P.; Rojas Plana, D.; Lammers, K.; Rubio Rodríguez, M.A. An Energy System Model-Based Approach to Investigate Cost-Optimal Technology Mixes for the Cuban Power System to Meet National Targets. *Energy* **2024**, *306*, 132492. [CrossRef]
40. Soler-Castillo, Y.; Rimada, J.C.; Hernández, L.; Martín Criado, G. Modelling of the Efficiency of the Photovoltaic Modules: Grid-Connected Plants to the Cuban National Electrical System. *Sol. Energy* **2021**, *223*, 150–157. [CrossRef]
41. Luukkanen, J.; Saunders Vázquez, A.; Majanne, Y.; Korkeakoski, M. Possibilities and Challenges of Developing a 100% Renewable Electricity System in Cuba. *Ing. Energética* **2023**, *44*, 1–11.
42. Alvarez, E.A.; Korkeakoski, M.; Santos Fuentefría, A.; Filgueiras Sainz de Rozas, M.L.; Arcila Padura, R.; Luukkanen, J. Long-Range Integrated Development Analysis: The Cuban Isla de la Juventud Study Case. *Energies* **2021**, *14*, 2865. [CrossRef]
43. Álvarez González, A.L.; Iturralde Carrera, L.A.; Jiménez Borges, R.; Monteagudo Yanes, J.P.; Gómez Muñoz, M. Potencialidades de generación fotovoltaica sobre cubiertas de edificaciones en una instalación hotelera. *Rev. Univ. Y Soc.* **2022**, *14*, 565–573.
44. Hernández Morales, C.; Monteagudo Yanes, J.P.; Edmilson Dala, H.; Jiménez Borges, R. Anteproyecto de sistema solar fotovoltaico en hotel universitario de posgrado en la universidad de Cienfuegos. *Rev. Univ. Soc.* **2020**, *12*, 163–169.
45. Iturralde Carrera, L.A.; Jiménez Borges, R.; Molina Santana, E.; Álvarez González, A.L. Potencialidades de generación fotovoltaica sobre la cubierta del edificio CRAI de la Universidad de Cienfuegos. *Rev. Univ. Y Soc.* **2022**, *14*, 318–330.
46. Castillo Alvarez, Y.; Magariño Abrahans, Y.; Jiménez Borges, R.; Iturralde Carrera, L.A.; Rodríguez Pérez, B.; Cruz-Pérez, M.Á.; Rodríguez-Reséndiz, J. Technical, Economic, and Environmental Assessment of Hybrid Solar Photovoltaic–Thermal Systems in Hospitals: A Comprehensive Climate Change Mitigation Strategy. *Eng* **2026**, *7*, 85. [CrossRef]
47. Jiménez Borges, R.; Castillo Alvarez, Y.; Iturralde Carrera, L.A.; Garduño Aparicio, M.; Rodríguez Pérez, B.; Rodríguez-Reséndiz, J. Methodological Framework for the Integrated Technical, Economic, and Environmental Evaluation of Solar Photovoltaic Systems in Agroindustrial Environments. *Technologies* **2025**, *13*, 360. [CrossRef]
48. Yahir, C.B.C.; Alberto, A.Y.F.; Yoisdel, C.A.; Reinier, J.B.; Angel, I.C.L.; Berlan, R.P.; Álvarez-Alvarado, J.M.; Juvenal, R.R. Integrated Assessment of Photovoltaic Systems in Multi-Family Buildings as a Strategy for Climate Change Mitigation and Urban Energy Sustainability. *Resources* **2026**, *15*, 70. [CrossRef]
49. Rodríguez Chávez, M.L.; Jiménez Borges, R.; Castillo Alvarez, Y.; Iturralde Carrera, L.A.; Álvarez González, A.L. Propuesta de un sistema solar fotovoltaico para la reducción del consumo de energía en una planta incubadora. *Rev. Univ. Soc.* **2023**, *15*, 52–58.
50. International Energy Agency. Emissions Factors 2025: CO_2 Emission Factors from Electricity and Heat Generation. 2025. Available online: https://www.iea.org/data-and-statistics/data-product/emissions-factors-2025 (accessed on 21 July 2026).
51. Intergovernmental Panel on Climate Change. *2006 IPCC Guidelines for National Greenhouse Gas Inventories, Volume 2: Energy*; Institute for Global Environmental Strategies (IGES): Hayama, Japan, 2006.
52. Carnevale, E.; Lombardi, L.; Zanchi, L. Life cycle assessment of solar energy systems: Comparison of photovoltaic and water thermal heater at domestic scale. *Energy* **2014**, *77*, 434–446. [CrossRef]
53. Kaapanda, H.N. Anteproyecto de Sistema Fotovoltaico y Térmico para la Residencia de Postgrado de la Universidad de Cienfuegos. Master's Thesis, Universidad de Cienfuegos "Carlos Rafael Rodríguez", Cienfuegos, Cuba, 2018.
54. Dibene-Arriola, L.M.; Carrillo-González, F.M.; Quijas, S.; Rodríguez-Uribe, M.C. Energy Efficiency Indicators for Hotel Buildings. *Sustainability* **2021**, *13*, 1754. [CrossRef]
55. Mengual Torres, S.G.; May Tzuc, O.; Aguilar-Castro, K.M.; Castillo Téllez, M.; Ovando Sierra, J.; Cruz-y Cruz, A.R.; Barrera-Lao, F.J. Analysis of Energy and Environmental Indicators for Sustainable Operation of Mexican Hotels in Tropical Climate Aided by Artificial Intelligence. *Buildings* **2022**, *12*, 1155. [CrossRef]
56. Nielsen, E.; Furbo, S.; Fan, J. Comparison of domestic hot water production with photovoltaic panels and solar thermal collectors. *Sol. Energy* 2026, *in press*. [CrossRef]
57. El Mardi, M.; Allouhi, A.; Rami, Y.; Tabet Aoul, K.A. Cost-effective and sustainable heating solutions for indoor swimming pools: A comparative study and LCOH assessment of PV-heat pumps and solar thermal collectors. *Energy Nexus* 2025, *in press*. [CrossRef]
58. Braimakis, K. Comparative techno-economic assessment of solar district heating architectures based on combined solar thermal collectors, heat pumps, PVs and batteries. *Appl. Therm. Eng.* **2025**, *281*, 128723. [CrossRef]
59. Mathebula, J.; Mbuli, N. Application of TOPSIS for multi-criteria decision analysis (MCDA) in power systems: A systematic literature review. *Energies* **2025**, *18*, 3478. [CrossRef]
60. Calise, F.; Figaj, R.D.; Vanoli, L. Energy and economic analysis of energy savings measures in a swimming pool centre by means of dynamic simulations. *Energies* **2018**, *11*, 2182. [CrossRef]

61. Kong, R.; Deethayat, T.; Asanakham, A.; Kiatsiriroat, T. Performance and economic evaluation of a photovoltaic/thermal (PV/T)-cascade heat pump for combined cooling, heat and power in tropical climate area. *J. Energy Storage* **2020**, *30*, 101507. [CrossRef]
62. Calise, F.; Dentice d'Accadia, M.; Figaj, R.D.; Vanoli, L. A novel solar-assisted heat pump driven by photovoltaic/thermal collectors: Dynamic simulation and thermoeconomic optimization. *Energy* **2016**, *95*, 346–366. [CrossRef]
63. Pater, S. Increasing energy self-consumption in residential photovoltaic systems with heat pumps in Poland. *Energies* **2023**, *16*, 4003. [CrossRef]
64. Pinamonti, M.; Prada, A.; Baggio, P. Rule-based control strategy to increase photovoltaic self-consumption of a modulating heat pump using water storages and building mass activation. *Energies* **2020**, *13*, 6282. [CrossRef]